Polymer 50 (2009) 4122–4127

Contents lists available at ScienceDirect

Polymer

journal homepage: www.elsevier.com/locate/polymer

Effect of spatial confinement on the development of β phase of polypropylene

Xue-Gang Tang [a], Wei Yang [b,*], Rui-Ying Bao [b], Gui-Fang Shan [b], Bang-Hu Xie [b], Ming-Bo Yang [b], Meng Hou [a,**]

[a] Division of Mechanical Engineering, School of Engineering, The University of Queensland, QLD 4072, Australia
[b] College of Polymer Science and Engineering, Sichuan University, State Key Laboratory of Polymer Materials Engineering, Chengdu, 610065 Sichuan, China

ARTICLE INFO

Article history:
Received 2 April 2009
Received in revised form
29 May 2009
Accepted 15 June 2009
Available online 23 June 2009

Keywords:
Spatial confinement
β Phase
Dynamically vulcanized PP/EPDM (TPV)

ABSTRACT

The focus of this study was the effect of spatial confinement on the development of nucleating agent-induced β phase polypropylene (PP) in the dynamically vulcanized thermoplastic elastomers (TPVs) based on dynamically vulcanized PP/ethylene-propylene-diene rubber (EPDM) blend. The melting behaviors, crystalline structures and the morphologies of the blends were studied by differential scanning calorimetry (DSC), wide-angle X-ray diffraction (WAXD) and scanning electron microscopy (SEM). The results indicate that the EPDM phase undergoes a series of changes from the dispersed phase to a continuous one, and again to the dispersed phase with increased content of curing agent, and the PP component always shows itself in a continuous phase. In this process, with the content of the nucleating agent unchanged, the content of β phase PP in the blends initially increases a little and then decreases with increasing PF (Phenolic resin) content. We believe spatial confinement provides a good explanation for the development of β phase PP.

1. Introduction

Isotactic polypropylene (iPP) is a polymorphic material, which has at least four modifications of crystals: mono-clinic(α), hexagonal(β), triclinic(γ) and smectic [1–4]. Since Padden and Keith classified the crystal forms of iPP [1], studies on the formation, microstructure and morphology of the β phase have attracted a great deal of interest. The β phase is thermodynamically metastable and difficult to achieve under normal processing conditions. PP rich in β-phase can only be obtained by special techniques such as crystallization at high undercooling [1,5], crystallization in temperature gradients [6–8], crystallization in shear fields [9–13], and crystallization with the aid of specific nucleating agent (NA) [14–16]. β phase PP (β-PP) has peculiar thermal and mechanical properties such as lower crystal density, melting temperature and fusion enthalpy, but higher heat distortion temperature, and especially higher impact strength than α-form PP [9,17,18].

At the same time, many investigations dealt with iPP in polymer blends [9,10,19–23]. Varga et al. [9,21] have summarized the factors influencing the formation of β-PP in blends of β-PP with other polymers. iPP-based polymer blends can be prepared without any difficulty if the other component is amorphous polymer, e.g., elastomer [10,19]. In the case of β-PP blending with other semi-crystalline polymers, β-PP is easily obtained if the other polymer component has no or negligible α-nucleating ability, such as low-density polyethylene (LDPE) [10,20]. Semi-crystalline polymers additive having α-nucleating ability do not suppress the formation of β-PP matrix if they can remain in a molten state during the crystallization process of the PP component [20,21].

Thermoplastic vulcanizates, or TPVs, are blends where the elastomer component is vulcanized in situ during melt mixing with the thermoplastic component at high shear and elevated temperature. Dynamic vulcanization of the elastomer component in a TPV enables the cross-linked elastomer, or rubber, to become the dispersed phase even in cases where the elastomer is the majority component, or its volume fraction is greater than 0.5. The raised viscosity of the elastomer owing to the vulcanization affects the phase continuity and promotes the phase inversion, i.e. the majority phase becomes the dispersed phase [24–26].

It is well known that morphology is a key determinant of the final properties of polymer blends, so it is interesting how the change in morphology affects the development of β-PP. This information can lead to the essence of the development of β-PP in polymer blends and guide us to design and prepare PP-based high performance materials. However, to the best of our knowledge, there has been no prior attention to this topic. So in this work, we introduced β nucleating agent (β-NA) into dynamically vulcanized TPV based on PP/EPDM blends to generate the β-PP, and studied the effect of the morphology of the blend on the development of β-PP.

* Corresponding author. Tel./fax: +86 28 8546 0130.
** Corresponding author.
E-mail addresses: ysjsanjin@163.com (W. Yang), m.hou@uq.edu.au (M. Hou).

0032-3861/$ – see front matter © 2009 Elsevier Ltd. All rights reserved.
doi:10.1016/j.polymer.2009.06.035

The TPV was prepared using the curing agent, phenolic resin, which reacts with EPDM alone and does not induce the degradation of PP, because of the absence of unsaturation [27].

2. Experimental section

2.1. Materials

We used the following materials;

1. The β nucleating agent (β-NA) used in this study was WBG-II, a powder composed of rare-earth organic compounds, which was purchased from Guangdong Weilinna Functional Material Company Ltd.;
2. iPP, with the trademark F401, a resin obtained from Lanzhou Petrochemical Company Ltd., has the following properties provided by manufacturer:
   a. MFR = 2.5 g/10 min according to ASTM D1238.79;
   b. density = 0.91 g cm^{-3} according to ASTM D1505-68; and
   c. a tacticity of 98%.
3. EPDM (Nordel 4725p) obtained from Dupont Dow Elastomers L.L.C., Wilmington, DE, USA., has these properties:
   a. contains 70% ethylene and 4.9% ENB (Ethylidene norbornene), with
   b. a Mooney viscosity ($ML^{125\,^{\circ}C}_{2+10}$); and
   c. $\overline{M}_w$ of 25 and 135 000 g/mol, respectively.
4. Phenolic resin (PF) obtained from Yuantai Biochemistry industry Company Ltd., with the trade mark TXL-201, and its properties are:
   a. Softening point at 75–95 °C;
   b. The content of methylol 6.0–7.5%;
   c. The content of water ≤1.0%; and
   d. The content of bromine ≤4.0%.

2.2. Sample preparation

The melt-reactive blending process for preparing TPV samples (PP:EDPM = 5:5 wt%) was carried out in an SHJ-20 co-rotating twin-screw extruder with a screw diameter of 25 mm, a length/diameter ratio of 23, and a temperature profile of 170, 180, 190, and 185 °C from the feeding zone to the die. The content of β-NA was 0.3 wt% (to the weight of the blends). The PF content is 0, 1, 2, 4, and 6 wt% (to the weight of the blends). PP, EPDM, PF, and β-NA were simply mixed first, and then added to the twin-screw extruder. The extrudate was then pelletized.

For the sake of brevity, the different TPVs with different PF dosage were designated as:

1. TPV1 (0 wt%);
2. TPV2 (1 wt%);
3. TPV3 (2 wt%);
4. TPV4 (4 wt%);
5. TPV5 (6 wt%) respectively.

Here, the TPV1 is not a thermoplastic vulcanizate because it was not cross-linked, while for convenience, in this paper, we still designated the PP/EPDM blend without PF as TPV1, and its cross-linking degree is zero.

The pellets were then dried and injection-molded into dumb-bell tensile samples and impact samples on a PS40E5ASE precise injection-molding machine, with a temperature profile of 170, 190, 200, and 195 °C from the feeding zone to the nozzle. Both the injection pressure and the holding pressure were 37.4 MPa. The samples so obtained were heat pressed for 10 min at a temperature of 200 °C and a pressure of 10 MPa in an XLB-D 400 × 400 × 2 compression molding machine into 1 mm thick sheet. The compression molded sheet was then cooled to room temperature under pressure.

2.3. Tests

2.3.1. Differential scanning calorimetry (DSC)

The samples were studied by means of a TA Q20 differential scanning calorimeter. In the tests, samples of about 5 mg were heated to 200 °C at a rate of 10 °C/min under a nitrogen atmosphere and held at 200 °C for 5 min to eliminate the thermal history. Afterward, the samples were cooled to 20 °C at a rate of 10 °C/min, staying about 3 min at 20 °C, and then heated again to 200 °C at a heating rate of 10 °C/min. The temperature and heat flow scales were calibrated using the melting of high-purity indium and zinc samples before testing.

2.3.2. Wide-angle X-ray diffraction (WAXD)

WAXD measurement was carried out with a DX-1000 X-ray diffractometer at room temperature. Before testing, the samples were heated up to 200 °C at a rate of 10 °C/min under a nitrogen atmosphere and held there at 200 °C for 5 min to eliminate anisotropy. Afterward, the samples were cooled to room temperature at a rate of 10 °C/min. The Cu K-alpha (wave length = 0.154056 nm) irradiation source was operated at 50 kV and 30 mA. The patterns were recorded by monitoring the diffractions from 5° to 50°, and the scanning speed was 3°/min.

The relative content of β-phase (K_β) in these samples was calculated from the WAXD diffractograms according to the following relation suggested by Turner Jones et al. [28],

$$K_\beta = \frac{H^\beta_{300}}{H^\alpha_{110} + H^\alpha_{040} + H^\alpha_{130} + H^\beta_{300}} \quad (1)$$

where H^α_{110}, H^α_{040}, H^α_{130} are the intensity of the (110), (040), and (130) reflections of α-phase, appearing at 2θ around 14.1°, 16.9°, 18.5°, respectively, and H^β_{300} is the intensity of (300) reflection of β-phase at 2θ around 16.0°. Here, all the diffraction data were corrected for background (air and instrument) scattering before analysis. The diffraction patterns were analyzed using MDI Jade 5.0 software (Materials Data Inc, Liverpool, CA).

2.3.3. Scanning electron microscope (SEM)

The phase morphology was examined using an OXFORD 6650 scanning electron microscope (SEM). Before testing, the same heat treatment as that for WAXD measurements was performed. To create better contrast, the samples were cryogenically fractured in liquid nitrogen and etched by xylene to extract the EPDM phase. After the solvent volatilized completely, the surfaces were coated with a layer of gold to avoid charging before SEM observation. The accelerate voltage was 10 kV.

3. Results and discussion

3.1. SEM analysis

The phase morphology of dynamically vulcanized EPDM/PP blends prepared with different PF content as the curing agent is shown in Fig. 1. It is interesting to note that, for dynamically vulcanized EPDM/PP blend, the EPDM phase undergoes a series of changes from the dispersed phase to a continuous one, and again to the dispersed phase with increasing content of curing agent, and the PP component always shows itself in a continuous phase. For TPV1, the EPDM, in the shape of deformed fiber or ellipsoid, is

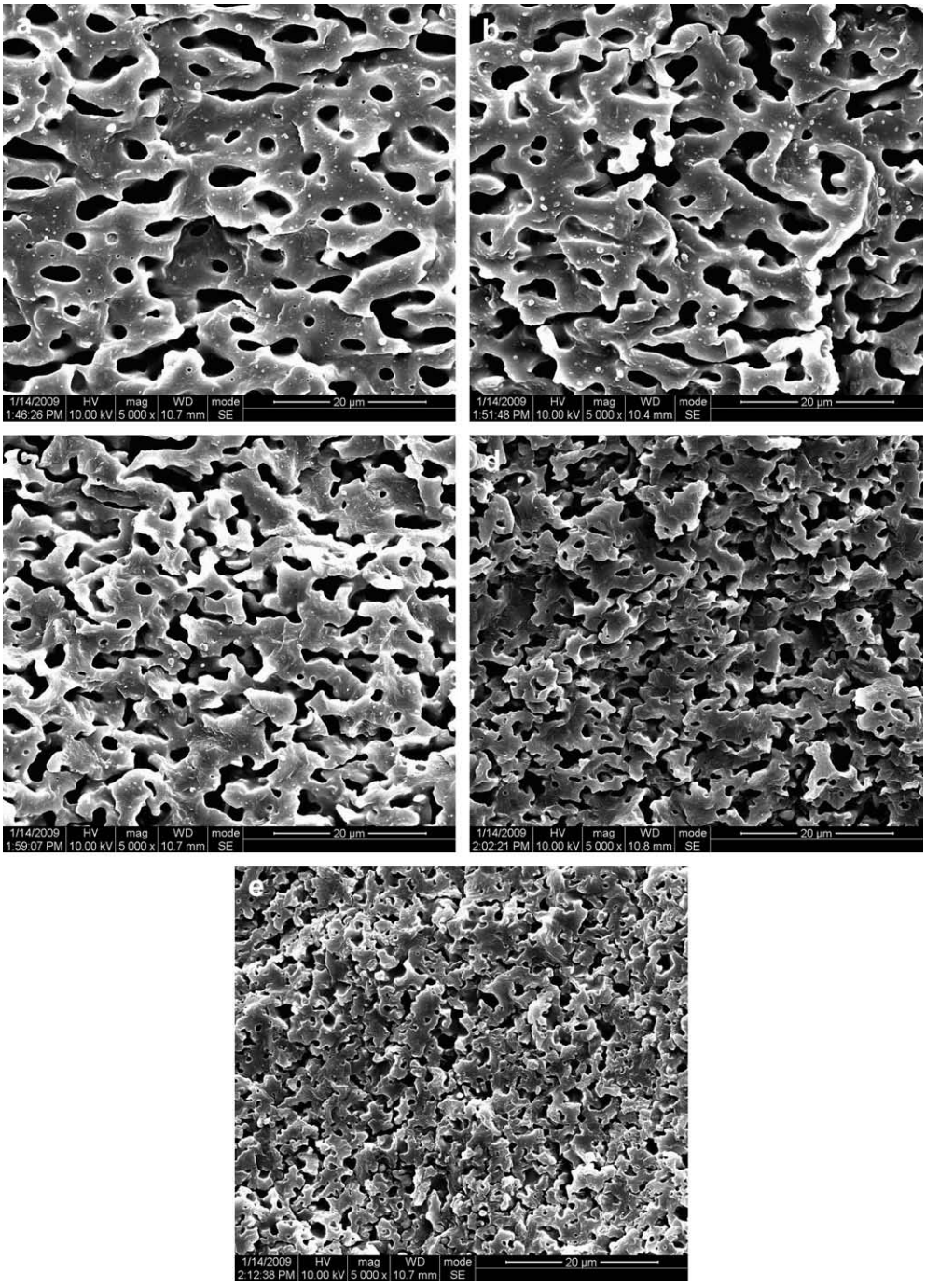

Fig. 1. SEM micrographs of TPVs with different PF content: (a) TPV1, (b) TPV2, (c) TPV3, (d) TPV4, (e) TPV5.

dispersed in the PP matrix. With increasing PF content (TPV2, TPV3, and TPV4), the blends show a co-continuous morphology. With further increases of the PF content (TPV5), the EPDM is dispersed again in the form of spherical droplets. A distinct change in the morphology of EPDM between TPV4 and TPV5, from the shape of deformed fiber liked structures to spherical droplets, can be noted.

Xiao et al. [29] reported similar phenomenon. In their study, during mixing the dispersion of EPDM in the blend mainly depends on both the viscosity difference between EPDM and PP and the interaction between EPDM particles. The former favors the formation of dispersed EPDM and the latter does not. When a small amount of curing agent is used, both the viscosity difference between EPDM and PP and the interaction between EPDM particles are increased. However, it may be that the effect of shear on the morphology of the blends is dominant and intense shear results in dispersion of EPDM particles in the blend. As the amount of curing agent increases, the interaction between EPDM particles is dominant, so EPDM particles aggregate easily and form a continuous phase. When a large amount of curing agent is incorporated, the viscosity difference between EPDM and PP plays the critical role, leading to the EPDM particles being immobilized by many cross links and breaking down into small droplets under the applied shear field. Under such conditions, the size of the EPDM particles decreases and was dispersed easily.

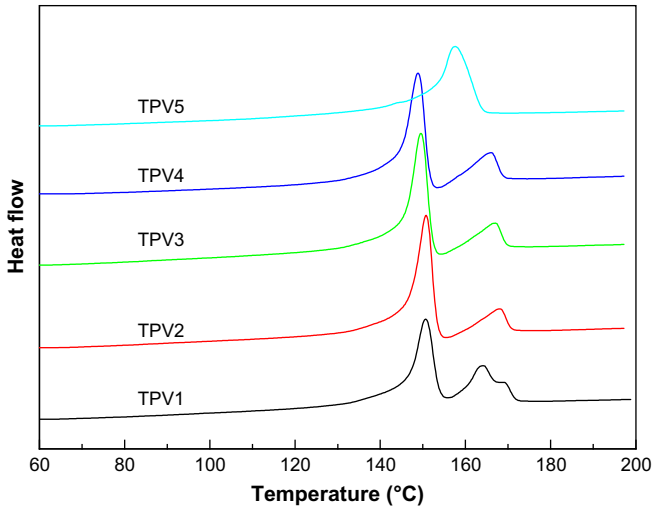

Fig. 2. Effect of PF content on the melting behaviors of TPVs.

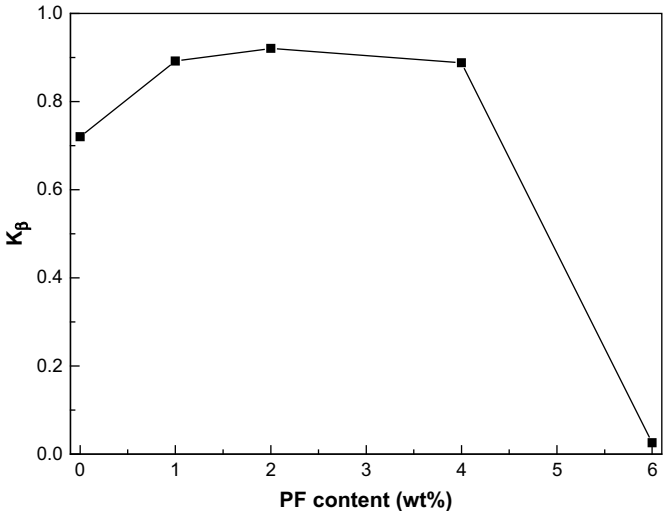

Fig. 4. Effect of PF content on the K_β value of TPVs.

3.2. Crystalline structures

Fig. 2 shows the melting behaviors of TPVs prepared with different PF content (after heat treatment). There are two melting peaks in the melting curves when the PF content is between 0% and 4% (wt), the lower temperature melting peak representing the characteristic peak of β-phase, and the higher temperature one representing that of α-phase. In this range, the temperature of the melting peak of β-phase decreases with the increasing PF content, which indicates that crystal perfection decreases. It is very interesting to note that there is only one melting peak located at 157.6 °C, a peak of α-phase of PP, when the content of PF is as high as 6 wt%, which means there is a sharp decrease of the content of β-PP formed at this PF content.

Fig. 3 show the WAXD patterns of the TPVs prepared with different PF content. The WAXD pattern of TPV1 shows a distinct peak at 2θ of about 16.0°, which corresponds to the (300) reflection of β-PP. At the same time, there are weak peaks appearing at 2θ of about 14.1, 16.8, 18.6, which correspond to the (110), (040), and (130) reflections of α-PP, respectively, indicating that the β-PP dominates in TPV1. For TPV2, TPV3, and TPV4, it can hardly distinguish the characteristic reflections of α-PP. While for TPV5, the case is completely reversed and only α-PP is present. It can be seen that there is not distinct reflection of α-PP in the WAXD test, while the melting characteristic peaks are found in DSC test for TPV2-TPV4 as shown in Fig. 1. This may result from re-crystallization during DSC test, which usually will forms α-PP [5].

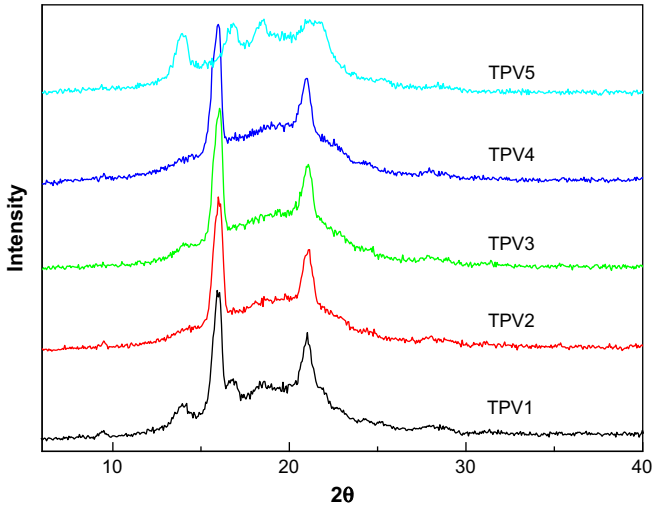

Fig. 3. WXRD patterns of TPVs with different PF content.

The dependence of the K_β value of the TPVs on the PF content is illustrated in Fig. 4, which indicates that the K_β value increases a little with increasing PF content, and then, sharply decreases when the PF content is 6 wt%.

Table 1 shows the size of the β-PP crystallites and the total crystallinity of all crystals calculated from the WAXD data. The crystallite sizes L_{hkl} in the direction perpendicular to (hkl) planes were estimated using the Scherrer equation, $L_{hkl} = \lambda/B\cos\theta$, where λ is the X-ray wavelength, B the reflection breadth at half-maximum, and 2θ the diffraction angle. To determine the crystallite sizes, the crystalline reflections (300) of β phase were selected. It can be seen that the total crystallinity of all crystals and the size of β crystallite remained almost constant, suggesting that the variation of PF content has almost no effect on the crystallite size and total crystallinity. The T_m of α phase and β phase both list in Table 2. It seems that with the increasing of the PF content, the T_m of α and β phase both decreases, which means the lowering of the crystal perfect of α phase and β phase.

Fig. 5 shows the effect of PF content on the crystallization temperature. It is interesting that the crystallization temperature changes a lot with increases of PF content, and the changing trend is almost the same as that of K_β, or the content of β phase. For TPV1–TPV4, the crystallization temperature is always above 120 °C, which corresponds to the crystallization temperature of β-PP, while for TPV5 when the content of PF is 6 wt%, the crystallization temperature is 114.07 °C, which is the crystallization temperature of α-PP [23]. These results show that the incorporation of PF leads to a change of crystallization temperature, especially when the content of PF is up to 6 wt%, and the crystallization temperature decreases to 114.07 °C, and makes the α phase dominate. So with

Table 1
Wide-angle X-ray diffraction data for TPVs with different contents of PF.

Sample	L_{300}(nm)	Total crystallinity (%)
TPV1 (0% PF)	15.1(0.8)	42.97
TPV2 (1% PF)	14.5(0.5)	40.03
TPV3 (2% PF)	15.2(0.5)	40.11
TPV4 (4% PF)	14.5(0.7)	42.68
TPV5 (6% PF)	0	44.23

Table 2
Thermal and crystallization data obtained from DSC for TPV with different PF content.

Sample	$T_{m\beta}$ (°C)	$T_{m\alpha}$ (°C)
TPV1	150.68	169.11
TPV2	150.79	168.22
TPV3	149.52	167.19
TPV4	148.89	166.22
TPV5	–	157.53

the incorporation of PF, the crystallization ability of β phase changes, resulting in the change of β phase content in the samples. At the same time, it can be seen in Table 1 that the total crystallinity remains almost constant, indicating there is competition between the development of α phase and β phase.

4. Discussion

The crystal structure of β-iPP, which was a "long-standing structural puzzle," has already been solved by Meille et al. [30] and Lotz et al. [31]. The β-PP has a trigonal unit cell with parameters $a = b = 1.101$ nm and $c = 0.65$ nm, containing three isochiral helices. It has been demonstrated that the lamellae structure of β phase is not organized in a cross-hatched but in a bundled structure [32–35]. Based on the study of the lamellae arrangement of α-PP and β-PP, Norton et al. [36] have pointed out that there are two possible growth mechanisms leading to the spherical symmetry, i.e.:

(a) Central multidirectional growth (category 1); and
(b) Sheaf-like unidirectional growth (category 2).

The β spherulites consisting of conventional smooth lamellae (i.e. without cross-hatching) develop through the sheaving mechanism, and the resulting spherulites are clearly of category 2. When cross-hatching is present, as in α spherulites, even in the absence of α nucleating foreign particle, the growth will be multidirectional. It is expected that the initial crystal will be a trellis structure of mutually orthogonal lamellae (such as can be observed in isolation from solution, the so called 'quadrites'). The continuing growth of the lamellae constituting the trellis structure, combined with some fanning and branching, will lead to a spherulite which conforms more closely to category l.

It is known that confinement will lead to orientation. Growth of large "spherulites" between a glass slide and a cover plate is restricted to the plane of the gap. Likewise, Waddon et a1. [37–39] have demonstrated that polymer crystallization between inorganic fibers in fiber-reinforced composites have their growth direction along the channel between the fibers. This leads to the surmise that whenever the growth of a normally spherulitic material can be confined to a narrow gap, only those growth orientations parallel to the gap will survive.

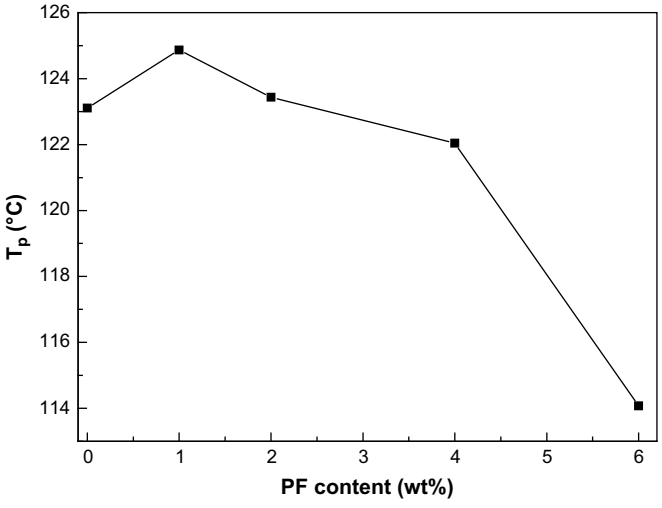

Fig. 5. Effect of PF content on the T_c (crystallization temperature) at the cooling rate of 10 °C.

At the same time, the orientation of the polymer chains in polymer blends has been extensively studied in past decades because of the possibility of producing unique orientation textures which cannot be formed in single-component polymeric materials. The oriented crystallization has been examined for some miscible crystalline/amorphous polymer blends [40–43]. Prud'homme et al. [40,41] studied the crystallization and orientation behavior of poly(ε-caprolactone) (PCL) in miscible blends with poly(vinyl chloride) (PVC) and reported that the crystallization under strain led to a crystalline orientation perpendicular to the strain direction under most conditions. Kaito et al. examined the oriented crystallization of an isotactic polystyrene (iPS)/poly(phenylene oxide) (PPO) blend and produced an orientation texture containing highly oriented iPS crystals and nearly isotropic PPO chains [42]. More recently, Park et al. [43] reported the oriented crystallization of poly[(R)-3-hydroxybutyrate] (PHB) in a blend with cellulose propionate (CP) that resulted in a change of the crystal orientation from *c*-axis-oriented growth to *a*-axis-oriented crystal growth by increasing the CP content. Kaito also studied the oriented crystallization of miscible crystalline/crystalline polymer blends, such as poly(1,4-butylene succinate)/poly(vinylidene fluoride) and poly-(vinylidene fluoride)/poly[(R)-3-hydroxybutyrate] [44,45]. The oriented crystallization in confined domains produces a new type of lamellar morphology, in which two components are segregated in nano-sized domains and are oriented in mutually opposite directions. There are many ways to form the confined domain, such as nano-rods or nano-tubes [46,47], block copolymer [48–50], and blend [44], and all of these will form nano-scale confinement structures, which will lead to the orientation of the molecular chains, and result in oriented crystals.

In this study, the morphology of EPDM changes greatly with increasing PF content. To better elucidate the morphologies, a schematic drawing of the structure of the TPVs with different PF content is shown in Fig. 6. For TPV1–TPV4, the EPDM phase shows a fiber-like or elliptical shape with a large aspect ratio, while for TPV5, the dispersed EPDM phase consists of droplets. Just like the nano-scale confinement to the molecular chains, for TPV1-TPV4, there is a strong morphology confinement in the micro-scale to the lamellae structures because of these fiber-liked structures, which will result in the orientation of the lamellae.

As well as this, there is another confinement, which can also result in the orientation of the lamellae. It is well known that most polymer blends are often phase-separated and thermodynamically

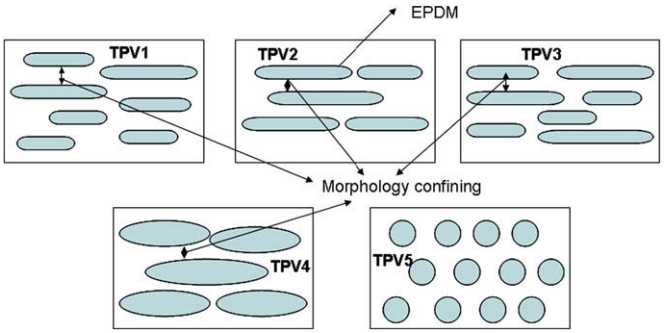

Fig. 6. The skeleton micrographs and analysis of TPVs with different PF content.

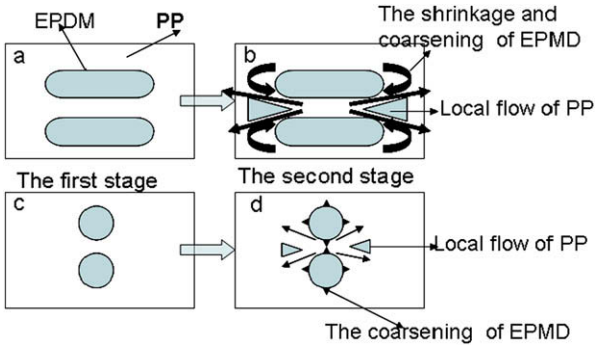

Fig. 7. The skeleton micrographs and detail analysis of TPVs with different shape of EPDM.

unstable. For example, under quiescent conditions, the domain size of the dispersed phase tends to increase with increasing time. At the same time, the deformed structure tends to shrink. The thermodynamic reason for these responses is a reduction of the interfacial area or interfacial energy [51–54]. So for the EPDM phase in the form of fiber or ellipsoid, the shrinkage trend during cooling will result in changes to the local flow field between the deformed structures.

Fig. 7 shows the detailed analysis of this kind of confinement exerted by the EPDM phase with different shapes. Here, Fig. 7a and c are the initial stages of different shapes of the EPDM phase. As time elapses, the second stage occurs. For Fig. 7b, in the region between the deformed structures, there is a compression force exerted by EPDM on PP because of the shrinkage and coarsening of EPDM, which will be helpful to the orientation of lamellae. For Fig. 7d, the situation is different, because there is just the coarsening effect, and the compression effect is very weak. These two kinds of confinements facilitate the orientation of lamellae. On a larger scale, the lamellae are organized in spherulites, densely branched, isotropic, polycrystalline superstructures – which give the final crystal structures.

As mentioned above, the growth mechanisms of α-PP and β-PP are different. The mechanism for β-PP is sheaf-like unidirectional growth, the lamellae of which will firstly grow along a particular direction, and then form spherulites, so the orientation of lamellae will contribute a lot to the development of β-PP. However, the mechanism for α-PP is central multidirectional growth, the lamellae of which will grow multidirectionally, so the orientation of lamellae will not contribute to the development of it, and may have an adverse effect.

With increasing PF content, changes of morphology mean that the strength of the spatial confinement increases a little from TPV1 to TPV4, while for TPV5, the strength of the spatial confinement becomes very weak. All of these are coincident very well with the changing trend of β-PP content, so the evolution of phase morphology of the blends resulting from different dosages of PF leads to the different crystallization ability of the matrix PP, and different content of β-PP.

5. Conclusion

This research have investigated the effect of PF content on the development of β-phase PP in dynamically-vulcanized TPV based on PP/EPDM blends, which showed that the formation of β-phase affected by PF content resulted in morphology change. With increasing PF content, the β-PP increased a little at first, and then decreased, and especially when the content of PF is 6%, the formation of β-phase is completely restrained. The phase morphology also experienced a series of changes with increasing PF content: the EPDM phase undergoes a change from the dispersed phase to a continuous one, and again to dispersed phase, and the PP component always shows itself in a continuous phase. This evolution of phase morphology resulted in the change of spatial confinement which significantly affects the development and final content of β-PP in the blends.

Acknowledgements

The authors gratefully acknowledge the financial support of National Natural Science Foundation of China (Grant No. 20734005), the Program for New Century Excellent Talents in University, Doctoral Research Foundation granted by the National Ministry of Education, China (Grant No. 20060610029), the Special Funds for Major Basic Research of China (Grant No. 2005CB623808) and the support from IPRS (International Postgraduate Research Scholarship, Australia). We are also heavily indebted to Mr. Zhu Li from Center of Analysis and Test of Sichuan University for careful SEM observation, and the editing work from Mr. Simon.

References

[1] Padden FJ, Keith HD. J Appl Phys 1959;30:1479.
[2] Turner-Jones A, Cobbold AJ. J Polym Sci 1968;B6:539.
[3] Meille SV, Bruckner S, Porzio W. Macromolecules 1990;23:4114.
[4] Lotz B, Graff S, Straupe C, Wittmann JC. Polymer 1991;32:2902.
[5] Varga J. J Macromol Sci Part B Phys 2002;41:1121.
[6] Crissman JM. J Polym Sci 1969;7:389.
[7] Lovinger AJ, Chua JO, Gryte CC. J Polym Sci Polym Phys Ed 1977;15:641.
[8] Varga J, Ehrenstein GW. Polymer 1996;37:5959.
[9] Varga J. Angew Makromol Chem 1983;112:191.
[10] Varga J. J Thermal Anal Calorim 1989;35:1891.
[11] Varga J, Karger-Kocsis. J Mater Sci Lett 1994;13:1069.
[12] Wang Y, Meng K, Hong S, Xie XM, Zhang CG, Han CC. Polymer 2009;50:636.
[13] Huo H, Jiang SC, An LJ. Macromolecules 2004;37:2478.
[14] Garbarczyk J, Paukzta D. Polymer 1981;22:562.
[15] Kotek J, Raab M, Baldrian J, Grellmann WJ. J Appl Polym Sci 2002;85:1174.
[16] Zhao S, Cai Z, Xin Z. Polymer 2008;49:2745.
[17] Karger-Kocsis J. Polym Bull 1996;37:119.
[18] Karger-Kocsis J. Polym Eng Sci 1996;36:203.
[19] Varga J, Garzó G. Angew Makromol Chem 1990;180:15.
[20] Varga J, Schulek-Tóth F, Mudra I. Macromol Symp 1994;78:229.
[21] Menyhárd A, Varga J. Eur Polym J 2006;42:3257.
[22] Tang XG, Yang W, Shan GF, Xie BH, Yang MB, Fu Q. J Macromol Sci Part B Phys 2007;46:841.
[23] Tang XG, Bao RY, Yang W, Xie BH, Yang MB, Hou M. Eur Polym J 2009;45:1448.
[24] Paul DR, Barlow JW. J Macromol Sci Rev Macromol Chem Phys 1980;C18:109.
[25] Metelkin VI, Blekht VS. Kolloid Zh 1984;46:476.
[26] Ultracki LA. J Rheol 1991;35:1615.
[27] van der Val A, Mulder JJ, Oderkerk J, Gaymans RJ. Polymer 1998;39:6781.
[28] Turner Jones A, Aizlewood JM, Beckett DR. Makromol Chem 1964;75:134.
[29] Xiao HW, Huang SQ, Jiang T. J Appl Polym Sci 2004;92:357.
[30] Meille SV, Ferro DR, Brückner S, Lovinger AJ, Padden FJ. Macromolecules 1994;27:2615.
[31] Lotz B, Kopp S, Dorset D. Sur une structure cristalline de polymeres en conformation hélicoidale 31 ou 32. CR Acad Sci Paris 1994;319(Série II):187–92.
[32] Tjong SC, Shen JS. Polymer 1996;37:2309.
[33] Coulon G, Castelein G, G'Sell C. Polymer 1999;40:95.
[34] Li JX, Cheung WL, Chan CM. Polymer 1999;40:2089.
[35] Li JX, Cheung WL, Chan CM. Polymer 1999;40:3641.
[36] Norton DR, Keller A. Polymer 1985;26:704.
[37] Lhymn C, Schultz JM. Polym Compos 1985;6:87.
[38] Waddon AJ, Hill MJ, Keller A, Blundell DJ. J Mater Sci 1987;22:1773.
[39] Schultz JM. J Polym Sci Polym Phys 1992;30:785.
[40] Zhao Y, Keroack D, Prud'homme R. Macromolecules 1999;32:1218.
[41] Morin D, Zhao YR, Prud'homme R. J Appl Polym Sci 2001;81:1683.
[42] Dikshit AK, Kaito A. Polymer 2003;44:6647.
[43] Park JW, Doi Y, Iwata T. Macromolecules 2005;38:2345.
[44] Li YJ, Kaito A, Horiuchi S. Macromolecules 2004;37:2119.
[45] Kaito A. Polymer 2006;47:3548.
[46] Wu H, Wang W, Yang HX, Su ZH. Macromolecules 2007;40:4244.
[47] Steinhart M, Göring P, Dernaika H, Prabhukaran M, Gösele U. Phys Rev Lett 2006;97:027801.
[48] Sun YS, Chung TM, Li YJ, Ho RM, Ko BT, Jeng US. Macromolecules 2007;40:6778.
[49] Hsiao MS, Zheng JX, Leng SW. Macromolecules 2008;41:8114.
[50] Huang P, Zhu L, Guo Y, Ge Q, Jing AJ. Macromolecules 2004;37:3689.
[51] Crist B, Nesarikar AR. Macromolecules 1995;28:890.
[52] Grizzuti NO, Bifulco O. Rheol Acta 1997;36:406.
[53] Chesters AK. Trans IchemE 1991;69:259.
[54] Sundararaj U, Macosko CW. Macromolecules 1995;28:2647.